Double and Single Planar Wire Arrays on University-Scale Low-Impedance LTD Generator

Alla S. Safronova, *Member, IEEE*, Victor L. Kantsyrev, *Member, IEEE*, Michael E. Weller, *Member, IEEE*, Veronica V. Shlyaptseva, *Member, IEEE*, Ishor K. Shrestha, Mindy Y. Lorance, Maximillian T. Schmidt-Petersen, Austin Stafford, Matthew C. Cooper, Adam M. Steiner, *Student Member, IEEE*, David A. Yager-Elorriaga, *Student Member, IEEE*, Sonal G. Patel, Nicholas M. Jordan, *Member, IEEE*, Ronald M. Gilgenbach, *Life Fellow, IEEE*, and Alexander S. Chuvatin

***Abstract*— Planar wire array (PWA) experiments were performed on Michigan Accelerator for Inductive Z-pinch Experiments, the University of Michigan's low-impedance linear transformer driver (LTD)-driven generator (0.1 Ω, 0.5–1 MA, and 100–200 ns), for the first time. It was demonstrated that Al wire arrays [both double PWA (DPWA) and single PWA (SPWA)] can be successfully imploded at LTD generator even at the relatively low current of 0.3–0.5 MA. In particular, implosion characteristics and radiative properties of PWAs of different load configurations [for DPWA from Al and stainless steel wires with different wire diameters, interwire gaps, and interplanar gaps (IPGs) and for Al SPWA of different array widths and number of wires] were studied. The major difference from the DPWA experiments on high-impedance Zebra accelerator was in the current rise time that was influenced by the load inductance and was increased up to about 150 ns during the first campaign (and was even longer in the second campaign). The implosion dynamics of DPWAs strongly depends on the critical load parameter, the aspect ratio (the ratio of the array width to IPG) as for Al DPWAs on high-impedance Zebra, but some differences were observed, for low-aspect ratio loads in particular. Analysis of X-ray images and spectroscopy indicates that K-shell Al plasmas from Al PWAs reached the electron temperatures up to more than 450 eV and densities up to 2×10^{20} cm^{-3}. Despite the low mass of the loads, opacity effects were observed in the most prominent K-shell Al lines almost in every shot.**

***Index Terms*— K-shell radiation, Linear Transformer Driver (LTD), planar wire array (PWA), plasma pinch, shadowgraphy images, X-ray spectra and images.**

Manuscript received October 11, 2015; revised January 10, 2016; accepted February 10, 2016. Date of current version April 8, 2016. This work was supported by NNSA under DOE Cooperative Agreement DE-NA0001984. S. Patel was supported by Sandia National Laboratories. D. Yager-Elorriaga was supported by an NSF Graduate Fellowship. *(Corresponding author: Alla S. Safronova.)*

A. S. Safronova, V. L. Kantsyrev, V. V. Shlyaptseva, I. K. Shrestha, M. Y. Lorance, M. Schmidt-Petersen, A. Stafford, and M. C. Cooper are with the University of Nevada, Reno, NV 89557 USA (e-mail: safronovaalla@gmail.com; victor@physics.unr.edu; veronica@unr.edu; shresthaishor@yahoo.com; minylora@gmail.com; maximillian sp94@gmail.com; austins@unr.edu; mattcooper616@hotmail.com).

M. E. Weller was with the University of Nevada, Reno, NV 89557 USA, and is currently with the Lawrence Livermore National Laboratory, Livermore, CA 94550 USA (e-mail: weller4@llnl.gov).

A. M. Steiner, D. A. Yager-Elorriaga, S. G. Patel, N. M. Jordan, and R. M. Gilgenbach are with the University of Michigan, Ann Arbor, MI 48109 USA (e-mail: amsteine@umich.edu; dyager@umich.edu; sonalpa@umich.edu; jordann@umich.edu; rongilg@umich.edu).

A. S. Chuvatin is with the Laboratoire de Physique des Plasmas, Centre National de la Recherche Scientifique, École Polytechnique, Palaiseau 91128, France (e-mail: chuvatin@yahoo.com).

Color versions of one or more of the figures in this paper are available online at http://ieeexplore.ieee.org.

Digital Object Identifier 10.1109/TPS.2016.2538291

I. Introduction

FOR petawatt-class Z-pinch accelerators, a linear transformer driver (LTD)-driven accelerator allows achieving high current and high power in relatively modest configurations and, therefore, promises to be more efficient than the conventionally used Marx-driven accelerator [1]. LTD-based drivers are currently considered for many applications, including X-ray radiography, very high-current Z-pinch drivers, isentropic compression drivers, and Z-pinch inertial fusion energy [2]. Presently, there are 0.5-MA, 100-kV LTD cavities in a rep-rated operation at Sandia National Laboratories (SNLs) and an even larger, unique 1-MA LTD cavity operating in a single-shot mode at the University of Michigan (UM) [2]–[4]. SNL is investigating an advanced LTD design for a future generator called Z-300 that could produce 50 MA in a current rise time of 130 ns. The peak current would far exceed the existing 26-MA Marx generator design of the refurbished Z generator. The Z-300 generator is predicted to produce radiation yields up to 11 MJ with a conversion efficiency into X-rays of 23%.

Because there are almost no data on how wire arrays radiate on LTD-based 0.5–1-MA machines in the USA, it is very important to perform radiation and plasma physics studies on this new type of generator. We have chosen planar wire arrays (PWAs), because they are highly efficient X-ray radiators with unique implosion and radiative properties that we have studied in detail since 2005 on the high-impedance, university-scale Zebra generator (1 MA, rise time of 100 ns, and 1.9 Ω) [5]–[17].

Experimental details of the first experiments with PWAs on the UM's Michigan Accelerator for Inductive Z-pinch Experiments (MAIZE) LTD generator are given in Section II. Implosion characteristics of PWA experiments are presented and discussed in Section III, and the radiative properties of PWAs are discussed in Section IV. Finally, the conclusion is drawn in Section V.

II. Experimental Details

Recently, we successfully performed the first collaborative PWA experiments on the unique university-scale LTD generator at UM. It is the MAIZE facility that consists of an LTD capable of generating a 1-MA current at 100 kV across a low-inductance matched load with ∼100-ns rise

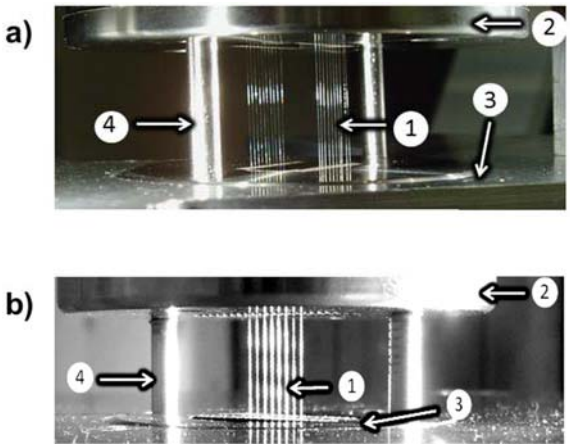

Fig. 1. PWA loads. (a) DPWA. (b) SPWA. 1: planar row of wires. 2: anode. 3: cathode. 4: supporting rod (removed before shot).

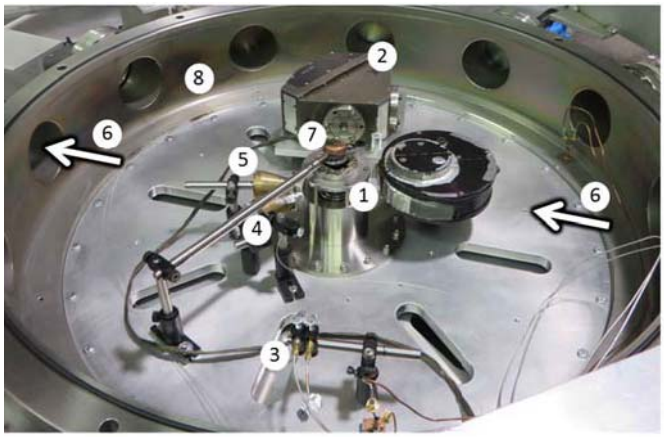

Fig. 2. MAIZE generator vacuum chamber (the diameter of 1 m) with diagnostics. 1: PWA load. 2: X-ray spectrometer with convex KAP crystal. 3: cluster of filtered Si diodes. 4 and 5: three-channel X-ray pinhole cameras. 6: laser-probing beam. 7: Faraday cup detector. 8: vacuum chamber.

time [3]. The first results of the experiments with the PWA were presented at the APS Annual meeting of Division of Plasmas Physics [18] and in this paper in more detail. The PWA experiments varied by array mass, which is controlled by the changes to the wire diameter, and by array configuration corresponding to the changes in interwire gap (IWG) and interplanar gap (IPG). In particular, two types of PWA loads, double PWA (DPWA) and single PWA (SPWA), were considered. The geometries tested are shown in Table I and Fig. 1. The major focus was on the experiments with DPWA, which consist of two parallel rows of wires and have demonstrated high radiation efficiency (up to 30 kJ), compact size (1.5–3 mm), and pulse shaping capabilities in the experiments at 1-MA Zebra accelerator [7], [9], [10], [13]. It was shown that their implosion dynamics strongly depends on the critical load parameter, the aspect ratio ϕ (array width to IPG) [9], [10]. In the first experiments on MAIZE, DPWA consisted of six wires (6/6) or eight wires (8/8) in each plane with IWG of 0.7 or 1 mm and IPG of 3 or 6 mm [see Fig. 1(a)]. The aspect ratio ϕ varied between 0.58 and 1.67. SPWA consisted of 12 wires with IWG of 0.7 mm [Fig. 1(b)]. Most of the PWA experiments were carried out with Al 5056 wires (95% Al and 5% Mg) and a few with stainless steel SS 304 wires (69% Fe, 19% Cr, and 9% Ni).

The diagnostic setup included laser shadowgraphy for the observation of plasma evolution at the early stages of plasma implosion. Different X-ray detectors and spectrometers that covered a spectral region of 1–10 keV were focused on the study of plasma properties near and at the stagnation stage, and a Faraday cup for the investigation of plasma electron beams (see Fig. 2).

The first campaign's laser-probing diagnostic was a two frame, 775-nm, 150-fs Ti:Sapphire laser shadowgraphy system with a 9-ns delay between frames. Later experiments utilized a four frame, 2-ns, frequency-doubled Nd:YAG laser.

A study of time history of X-ray yields was made using two Si-diodes AXUV-HS5 (0.7-ns time resolution) with aluminized 6-μm Mylar filters (the cutoff energy of 1.4 keV). For X-ray imaging, two time-integrated side-on pinhole cameras with the spatial resolution of 90 μm were used. The first and second cameras were oriented at the angles of 90° and 45° to the PWA's wire rows, respectively. Each of these X-ray pinhole cameras captured three plasma images using different filters with the cutoff energy of 1.4, 1.6, and 3.5 keV. The pinhole cameras recorded their images using Kodak Bio-max MS X-ray film (see Fig. 2).

Spectroscopic diagnostics was employed in order to estimate ion charge states, electron temperature and density, and opacity effects. We used a side-on time-integrated X-ray convex crystal spectrometer with a potassium acid phthalate (KAP) crystal (a radius of curvature of 51 mm) with the spatial 1-D axial resolution of 4 mm to record X-ray emission up to 12–14 Å. The second spectrometer with a LiF crystal (a radius of curvature 25.4 mm) has no spatial resolution and was used for the study of hard X-ray emission from plasma up to 2.3 Å. The 7.5-μm-thick kapton in combination with the aluminized 3-μm-thick Mylar (or 1-μm Mylar) filter was applied as the filters in both spectrometers.

A Faraday cup detector was utilized for electron beam-current measurements in these experiments. This detector was filtered with a 25-μm Cu filter to register electrons with energy more than 94 keV. The Faraday cup was placed at a fixed distance of 40 mm above the anode.

The LTD was limited to 70% of the maximum charge voltage to prevent damage to the capacitors from voltage ringback due to high load inductance (similar to the previous experiments with foils reported in [4]). As a result, the peak current was between 330 and 420 kA, and the rise time was between 136 and 179 ns (Table I).

III. Implosion Characteristics of Planar Wire Array Experiments on Maize at the University of Michigan

The implosions of Al PWAs of different load configurations were achieved, analyzed, and compared with the high-impedance Zebra generator results from the University of Nevada, Reno (UNR). For DPWAs, this included a broad range of aspect ratios ($\phi = 0.58$–1.67), and

TABLE I
LOAD CHARACTERISTICS, PEAK CURRENT, AND CURRENT RISE TIME IN DPWA AND SPWA EXPERIMENTS DURING THE JOINT UNR/UM CAMPAIGN ON THE UM'S MAIZE GENERATOR

MAIZE Shot N	Load configuration/ wire material and number of wires	Wire Diameter (μm)	Array Mass (μg/cm)	Inter-Wire Gap/ Inter-Planar Gap (mm)	Aspect Ratio Φ	Peak current (kA)	Current rise time (ns)
605	DPWA Al 5056 6/6	12.7	41	1 / 3	1.67	340	142
612	DPWA Al 5056 6/6	12.7	41	0.7 / 6	0.58	420	140
620	DPWA Al 5056 6/6	10	25	1 / 3	1.67	380	136
621	DPWA SS 304 8/8	5.1	26	1 / 3	1.67	400	161
622	SPWA Al 5056 12	10	25	0.7	N/A	330	143
623	DPWA Al 5056 6/6	10	25	0.7 / 6	0.58	390	152
931	DPWA Al 5056 6/6	10	25	0.7 / 6	0.58	360	179

for SPWAs, this included a variation in the array width and number of wires. The most informative shots are shown in Table I. The wire ablation dynamics model (WADM) [19] that was successfully applied many times to predict and describe the implosion characteristics of PWAs produced by our team in the experiments on Zebra at UNR [7]–[9] proved to be very useful in predicting and analyzing the PWA experiments on UM's MAIZE. The wire dynamics model considers the motion of the each wire in an arbitrarily arranged array in a self-consistent magnetic field, induced by all other wires as well as the return currents described by the dynamic equations [20]. The WADM is an upgrade of the original wire dynamics model and uses the same equation of motion of thin filaments carrying some currents but allows momentum redistribution between the ablating array wires and the ablated plasmas [19].

First, we will consider the implosion dynamics of DPWAs and then move to SPWAs. It was mentioned above that the implosion dynamics of DPWAs on Zebra strongly depends on the critical load parameter, the aspect ratio ϕ [10]. In particular, the type of DPWA implosion dynamics observed is a function of the global magnetic topography. The field penetration between planes can be described by the aspect ratio ϕ. DPWA loads with a very low ϕ ($\phi < 0.7$) allow the global magnetic field to penetrate to the central symmetry axis of the load and produce a potential saddle point between the planes. In this extreme case, the DPWA loses inductive coupling and behaves as two isolated SPWA loads [10]. In addition, there is no observable mass accumulation on axis during the wire ablation and, therefore, no primary precursor formation. This is shown in Fig. 3, where the WADM calculations of the plasma mass and current densities are shown for the low-aspect ratio DPWA load ($\phi = 0.58$) tested in MAIZE shot 612 with Al 5056 wires (mass = 41 μg/cm, 6/6, IWG = 0.7 mm, and IPG = 6 mm). In Fig. 4, the experimental data for this shot are displayed: experimental current (light gray region) and Si X-ray diode (dark gray region) signals along with shadowgraphy timing [Fig. 4(a)] as well as shadowgraphy images [Fig. 4(b) and (c)]. There are a few X-ray peaks indicating multiple implosion with peaks at 82 and 106 ns, which are earlier than predicted by WADM (154 ns).

Such early implosions can correspond to the independent implosions of each plane of DPWA, which usually occurs much earlier than the main implosion in the center between planes. Indeed, a comparison of WADM calculations and a shadowgraphy image at much earlier time (Fig. 3, 66 ns) shows a good match [Fig. 4(c)].

In addition, in Fig. 5, we present the implosion characteristics of another Al 5056 DPWA experiment with the same low-aspect ratio ($\phi = 0.58$) but of a lighter mass in MAIZE shot 931 that was carried out during the second campaign when the LTD was producing the longer implosions. The rise time in MAIZE shot 931 was 179 ns, which is 39 ns longer than in shot 612. The implosion was characterized by one single peak at 214 ns that was later than predicted by the WADM at 173 ns. However, the four-frame shadowgraphy images taken with improved quality (2-ns, 532-nm frequency-doubled Nd:YAG laser) during the second campaign capture implosion dynamics with remarkable details [Fig. 5(b)–(e)] that have not been observed in 100-ns rise time DPWA experiments on Zebra. The first frame taken at 102 ns displays independent implosion of two planes moving to the center and in some sense is similar to the shadowgraphy image in Fig. 4(c). However, the second frame at 112 ns displays the

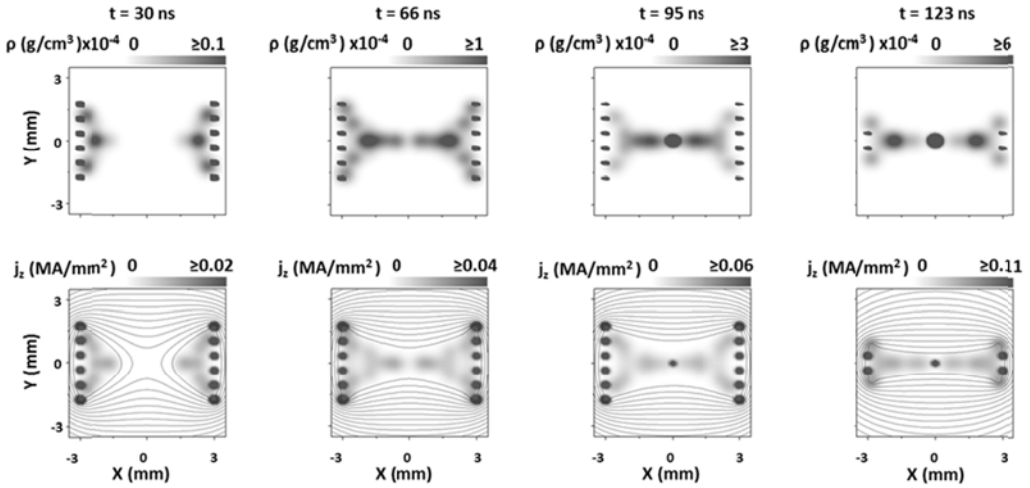

Fig. 3. Theoretical WADM calculations for the experimental configuration of MAIZE shot 612 (Al DPWA, 6/6, array mass = 41 μg/cm, IWG = 0.7 mm, IPG = 6 mm, and $\phi = 0.58$). The plasma mass density (top) and current density with magnetic field lines (bottom) at various timings.

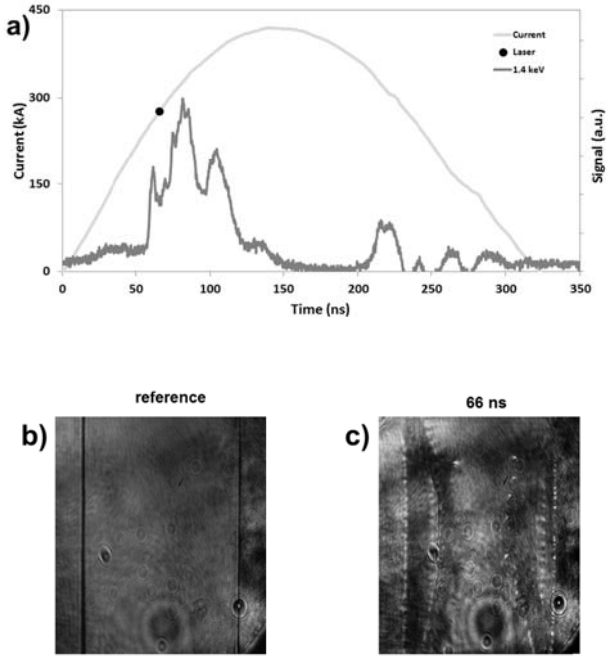

Fig. 4. Al DPWA in MAIZE shot 612. (a) Experimental current (light gray region) and Si diode (dark gray region) signals along with shadowgraphy timing (black dot). Shadowgraphy images recorded by 775-nm Ti:Sapphire laser at (b) preshot and (c) 66 ns after the current starts. The whole A–K gap of 1 cm (in the vertical direction) and the IPG of 6 mm (in the horizontal direction) are observed. Shadowgraphy with no precursor material in the center column, which correlates well with the mass density plotted in Fig. 3 at the same time, is shown in (c).

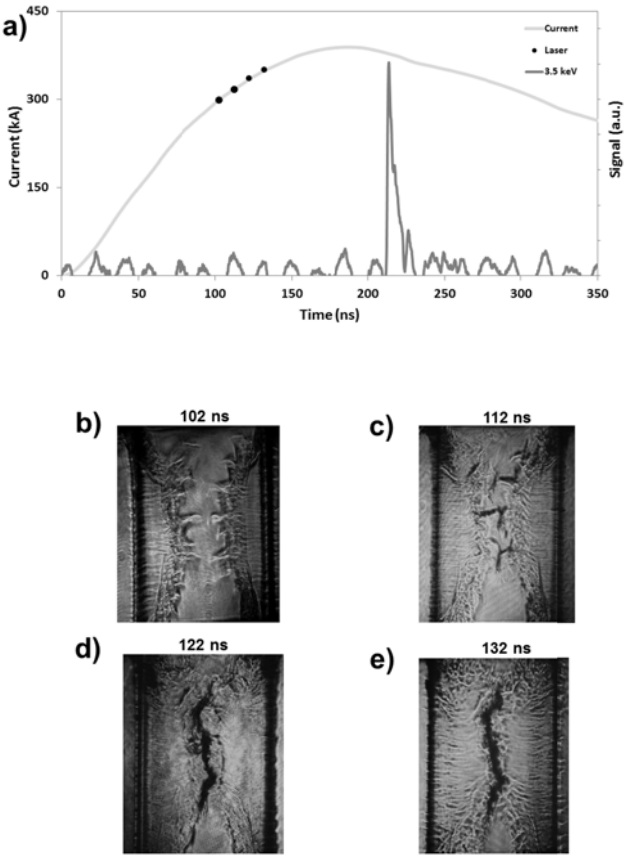

Fig. 5. Al DPWA in MAIZE shot 931. (a) Experimental current (light gray region) and Si diode (dark gray region) signals along with the shadowgraphy timing (black dots). Shadowgraphy images recorded by 532-nm Nd:Yag laser at (b) 102, (c) 112, (d) 122, and (e) 132 ns after the current starts. The whole A–K gap of 1 cm (in the vertical direction) and the IPG of 6 mm (in the horizontal direction) are observed.

moment when two independent plasma flows started to connect in the center (never captured before), and the following frames recorded at 122 and 132 ns show the primary precursor in the center that was never observed for low-aspect ratio loads.

As ϕ becomes very high ($\phi > 1.3$), the global magnetic field is effectively excluded from the interior of load. In such DPWAs, as the IPG closes, the load dynamics becomes similar to that of an SPWA, and produces an early axial precursor and, later, secondary precursors [7], [9], [10]. The high-aspect ratio DPWA load ($\phi = 1.67$) was tested in MAIZE shot 621 with stainless steel wires (8/8, array mass = 26 μg/cm, IWG = 1 mm, and IPG = 3 mm). In Fig. 6, the experimental data for this shot are displayed: experimental current (light gray region), Si X-ray diode (dark gray region),

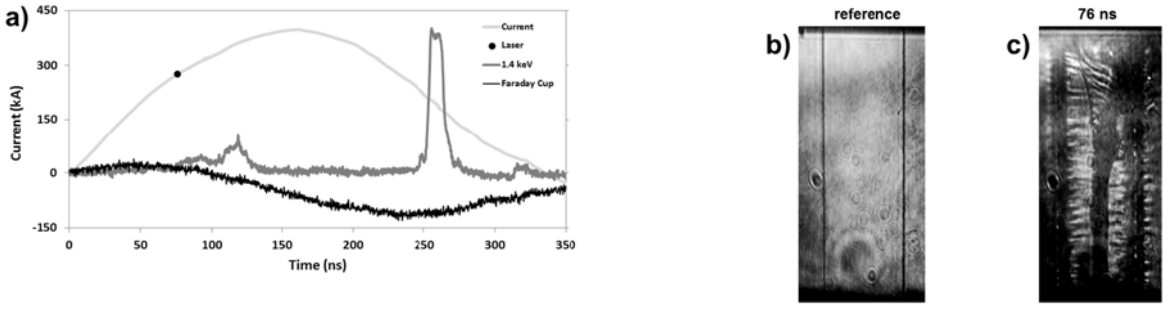

Fig. 6. SS DPWA in MAIZE shot 621. (a) Experimental current (light gray region), Si diode (dark gray region), and Faraday cup (black curve) signals along with the shadowgraphy timing (black dot). Shadowgraphy images recorded by 775-nm Ti:Sapphire laser at (b) preshot and (c) 76 ns after the current starts. The whole A–K gap of 1 cm (in the vertical direction) and the IPG of 3 mm (in the horizontal direction) are observed. Shadowgraphy that shows asymmetrical precursor material in the center column similar to the implosion of Al DPWA of the similar aspect ratio is shown in (c).

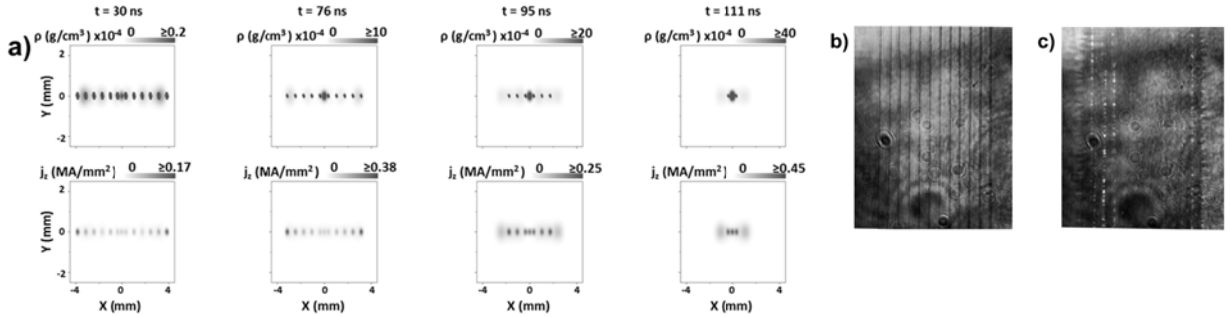

Fig. 7. Al SPWA in MAIZE shot 622 (12 wires, array mass = 25 μg/cm, and IWG = 0.7 mm). (a) Theoretical WADM plasma mass density (top) and current density (bottom) at various timings. Shadowgraphy images recorded by 775-nm Ti:Sapphire laser at (b) preshot and (c) 76 ns after the current starts. The whole A–K gap of 1 cm (in the vertical direction) and the array width of 7.7 mm (in the horizontal direction) are observed.

and Faraday cup (black curve) signals along with shadowgraphy timing [Fig. 6(a)] as well as shadowgraphy images [Fig. 6(b) and (c)]. The current rise time was 161 ns (the longest among DPWAs tested during the first campaign). There are two X-ray bursts at 124 ns (small intensity) and much later at 264 ns (largest intensity). The first X-ray diode signal peak is close to the WADM predictions of 139 ns. Such late implosion can be explained by the different ablation rates of stainless steel and not enough mass accumulation at the expected time of the implosion. The Faraday cup signal (which registers electrons with the energy more than 94 keV) reaches a maximum value near 250 ns, which correlates with the largest peak of the X-ray diode signal. The electron beam current in this shot, estimated from measuring the electron current on the collector of Faraday cup based on the amplitude of Faraday cup signal obtained from oscilloscope, was ~4.4 kA. It exceeds the values of electron beam current from Faraday cup measurements for most of Al DPWA loads in the first campaign. The detailed analysis of Faraday cup measurement results will be the subject of another paper. The shadowgraphy image displays different signatures (compared with the low-aspect ratio loads) as was expected. Indeed, the shadowgraphy recorded at 76 ns indicates a precursor in the center [Fig. 6(c)], which is supported by WADM and is almost independent of the wire material. For example, the shadowgraphy image in Fig. 6(c) closely resembles the shadowgraphy image recorded at 69 ns in the MAIZE shot 620 with Al DPWA of the identical load geometry (see Table I), not shown here.

Now, we discuss the implosion dynamics of SPWA using the results of the MAIZE shot 622 and WADM calculations (see Table I and Fig. 7). During the ablation phase, according to the WADM, the wires are involved in a cascade-type implosion starting with the outermost wires and ending with the innermost wires, which is shown in Fig. 7(a). In MAIZE shot 622, the current rise time was 143 ns (close to the average during the first campaign), and the maximum of the X-ray peak at 116 ns coincides very well with the WADM predictions of 118 ns (not shown here). In Fig. 7, the reference preshot frame clearly indicates 12 wires [Fig. 7(b)], while the shadowgraphy image recorded 76 ns later [Fig. 7(c)] shows no discrete wires in the middle. This agrees well with the WADM calculations at the corresponding time [Fig. 7(a) (second column)].

IV. Radiative Characteristics of Planar Wire Array Experiments on MAIZE at UM

As was mentioned above, the DPWA demonstrated the best radiation characteristics among the compact loads tested at 1-MA Zebra accelerator. One of the first and most studied DPWAs was from Al alloyed wires [5], [6], [9], [10], [12], [14]. Al plasmas produced in the implosions of Al wire arrays on 7-MA Saturn and 20-MA Z generators at SNL, and even on the university-scale generators, are almost always optically thick with respect to the K-shell emission of highly

charged Al ions, and thus, it is challenging to diagnose plasma conditions. A diagnostic method for studying radiation from such wire array implosions was suggested, successfully applied, and described in [21] and [22]. It is based on the use of the alloyed Al 5056 wires, which have 95% Al and 5% Mg. Mg K-shell lines are much less influenced by opacity because of their relatively low concentration and are, therefore, helpful in the diagnosis of optically thick K-shell plasmas. We have used the alloyed Al wires in the PWA experiments on both Zebra at UNR and MAIZE at UM. The most comprehensive analysis of radiative properties of both DPWAs and SPWAs from Al alloyed wires on 1-MA Zebra was described in [12]. In that work, electron temperature and density gradients in the axial direction, and in time, were estimated as well as opacity characteristics using non-local thermal equilibrium (non-LTE) kinetic models. In particular, the modeled plasma electron densities varied from 5×10^{18} cm^{-3} to 10^{20} cm^{-3} and electron temperatures between 300 and 420 eV [12]. The profiles of electron density and temperature were shown to change monotonically in the axial direction and in time. Time dependence of electron temperatures follows the X-ray diode signals. In general, the experiments with alloyed Al PWAs indicated that the Al plasmas are optically thick and become thicker near the stagnation phases. The modeling showed that the DPWAs have the highest optical depth of Al Heα line ($\sim$16) near the stagnation as well as the highest nonuniformity [12].

During the first experiments on MAIZE generator at UM, X-ray time-integrated spatially resolved (TISR) spectra in the spectral region of 4–16 Å as well as X-ray TISR pinhole images (filtered to provide the cutoff energy of 1.4 keV) were collected over a 1-cm distance from anode to cathode. Overall, the X-ray TISR pinhole images and spectra show regionalized K-shell Al and Mg radiation. Experimental spectra were compared with non-LTE kinetic modeling of K-shell Al and Mg spectra to estimate the plasma electron temperatures and densities as well as opacity effects. The non-LTE kinetic models of Al and Mg are based on the atomic data from Flexible Atomic Code (FAC) code [23] and are described in detail elsewhere [12], [14]. They are used to estimate plasma electron temperature and density of lineouts from TISR spectra, with each lineout corresponding to a particular distance from the anode. The most intense diagnostically important K-shell He-like and H-like resonance lines are: Al Heα at 7.758 Å ($1s2p^1P_1$–$1s^{21}S_0$), Al Lyα at 7.174 Å ($2p^2P_{1/2,3/2}$–$1s^2S_{1/2}$), Al Heβ at 6.635 Å ($1s3p^1P_1$–$1s^{21}S_0$), Al Heγ at 6.314 Å ($1s4p^1P_1$–$1s^{21}S_0$), Al Lyβ at 6.054 Å ($3p^2P_{1/2,3/2}$–$1s^2S_{1/2}$), Mg Heα at 9.17 Å ($1s2p^1P_1$–$1s^{21}S_0$), and Mg Lyα at 8.422 Å ($2p^2P_{1/2,3/2}$–$1s^2S_{1/2}$). Modeling of K-shell Al was focused on fitting the experimental spectral features with lines from high Rydberg states (such as Al Heβ, Al Heγ, and Al Lyβ) to minimize the influence of opacity effects.

The TISR spectra and pinhole image of the most massive DPWA (MAIZE shot 605) are shown in Fig. 8(a). The DPWA in this shot was configured to have a 1-mm IWG and a 3-mm IPG with the largest array mass of 41 μg. The TISR spectra and pinhole images correspond to a 1-cm distance from the anode to the cathode. Intense K-shell Al and Mg radiation is apparent near the cathode in the TISR spectra with significantly less radiation near the anode. Similarly, it is evident in the pinhole image that there is much more intense radiation near the cathode than the anode. Fig. 8(b) shows three experimental lineouts fit with theoretical modeling. As shown in Fig. 8(b), the modeling of the most prominent K-shell Al lines is overestimated, and the plasma parameters from K-shell Al and Mg are slightly different. The model assumes that the plasma is optically thin, so overestimations are an indication of opacity effects. In particular, such overestimations provide insight into the opacity of the plasma indicating that these prominent K-shell Al lines are optically thick. The K-shell Mg lines are not overestimated and are considered optically thin. K-shell Al modeling indicates electron temperatures at 400 eV and electron densities at 2×10^{20} cm^{-3}, whereas for K-shell Mg, the electron temperature is between 320 and 370 eV and the electron density of 2×10^{19}–1×10^{20} cm^{-3}.

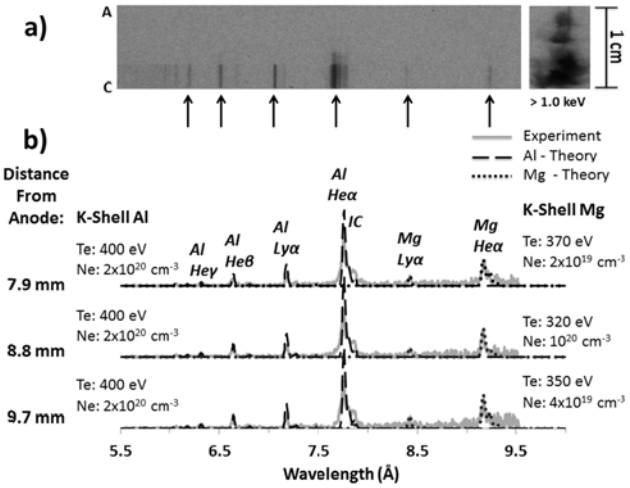

Fig. 8. Al DPWA in MAIZE shot 605 (6/6, array mass = 41 μg/cm, IWG = 1 mm, and IPG = 3 mm). (a) X-ray TISR spectra and pinhole image. Both images show nonuniform radiation with the most prominent radiation near the cathode. (b) Experimental lineouts of the TISR spectra fit with theoretical modeling.

Al DPWA in MAIZE shot 620 was of the same configuration as in shot 605, i.e., with wires composed of Al 5056 arranged with a 1 mm IWG and a 3 mm IPG, but of a much smaller array mass of 25 μg (not shown here). Similar to the spectra of Shot 605, it is apparent that there is significantly more intense radiation near the cathode than the anode in both the TISR spectra and the pinhole image (not shown here). Modeling of K-shell Al radiation indicates hotter plasmas, higher electron densities and stronger opacity effects.

The TISR spectra and pinhole image as well as the experimental lineouts and theoretical modeling of the TISR spectra from MAIZE shot 623 are shown in Fig. 9. The Al DPWA in this shot has the same array mass as in shot 620, but with a different configuration (smaller IWG of 0.7 mm and larger IPG of 6 mm). Non-LTE kinetic modeling of K-shell radiation from the TISR spectra indicates much hotter plasma near the

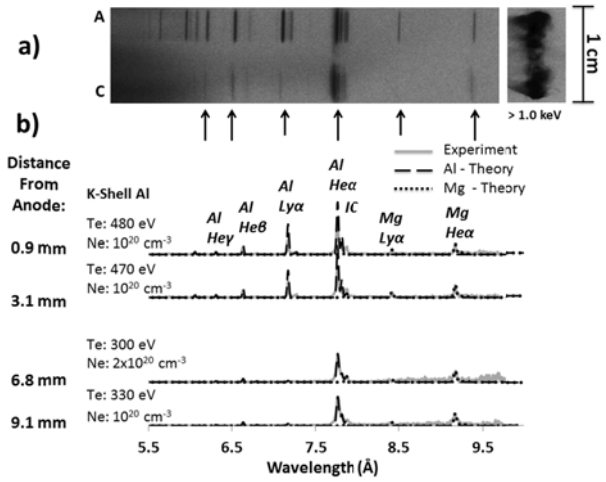

Fig. 9. Al DPWA in MAIZE shot 623 (6/6, array mass = 25 μg/cm, IWG = 0.7 mm, and IPG = 6 mm). (a) X-ray TISR spectra and pinhole image. Both images show nonuniform radiation with the most prominent lines near both cathode and anode. (b) Experimental lineouts of the TISR spectra fit with theoretical modeling.

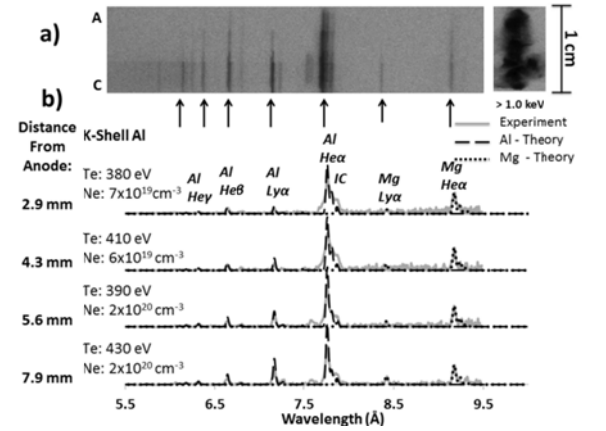

Fig. 10. Al SPWA in MAIZE shot 622 (12 wires, array mass = 25 μg/cm, and IWG = 0.7 mm). (a) X-ray TISR spectra and pinhole image. The most intense K-shell lines fill the whole A–C gap. (b) Experimental lineouts of the TISR spectra fit with theoretical modeling.

anode (470–480 eV) than near the cathode, unlike the modeling of shots 605 and 620, where intense K-shell radiation is predominantly near the cathode rather than near the anode. As shown in Fig. 9(b), closer to the anode, the most prominent K-shell Al lines are overestimated and optically thick. However, near the cathode, the K-shell Al lines are optically thin, and the results of both K-shell Al and Mg agree well with each other and indicate electron temperatures between 300 and 330 eV and electron densities near 2×10^{20} cm^{-3}.

The TISR spectra and pinhole image of the Al SPWA, MAIZE shot 622, are shown in Fig. 10(a). The SPWA had 12 Al 5056 wires with the IWG of 0.7 mm and an array mass of 25 μg. Both spectral images correspond to a 1-cm distance from anode to cathode. It is apparent that there is nonuniform K-shell radiation in the TISR spectra. There is significantly more intense radiation closer to the cathode than near the anode indicating cooler plasma near the anode. In addition, intense K-shell Al lines, as well as a He-like Mg line, were observed along the whole anode–cathode gap.

In contrast, for Al DPWAs most of the lines were localized either near the cathode or close to both the cathode and anode. Multiple lineouts of the TISR spectra of this SPWA have been modeled and compared, as seen in Fig. 10(b). The opacity effects were observed and overestimations of the K-shell Al lines were more uniform spatially than for Al DPWA. K-shell modeling indicates electron temperatures between 380 and 430 eV (the largest near the cathode) with electron densities between 6×10^{19} and 2×10^{20} cm^{-3}.

V. Conclusion

The first experiments on MAIZE LTD generator at UM demonstrated that the Al wire arrays (both DPWA and SPWA) can be successfully imploded even at the relatively low current of 0.3–0.5 MA. The major difference from the DPWA experiments on high-impedance Zebra accelerator was in the current rise time that was influenced by the load inductance and was increased up to about 150 ns during the first campaign (and was even longer at about 180 ns in the second campaign). The implosion dynamics of DPWAs indeed strongly depends on the critical load parameter, the aspect ratio ϕ (the ratio of the array width to IPG) as for Al DPWAs on high-impedance Zebra, but some differences were observed, for low-aspect ratio loads in particular. For high-aspect ratio DPWAs ($\phi = 1.67$), WADM predicts the implosion time and describes the implosion characteristics well. The global magnetic field is effectively excluded from the interior of load, and the IPG closes and produces an early axial precursor. This precursor was observed both in Al and stainless steel DPWA implosions on MAIZE generator. Interestingly, for the low-aspect ratio Al DPWAs, WADM described well the implosion characteristic only during the first 70 ns after the current starts and not later in time and was not able to predict the implosion time. Though no axial precursor and independent implosions of each plane was observed for the low-aspect ratio Al DPWA load on Zebra accelerator, shadowgraphy in MAIZE shot 931 (the current rise time of 179 ns) clearly shows the formation of the precursor at 122 ns, which stays unchanged for the next frame at 132 ns. One of the possible explanations is much longer implosions on MAIZE. Such evolution of the implosion and formation of the precursor could not be observed during the short 100-ns rise time of Zebra accelerator. However, WADM predicts well both implosion time and implosion characteristics of Al SPWA, which resembles the results on Zebra accelerator. X-ray imaging and spectroscopy demonstrated that the PWAs were imploded and K-shell Al plasmas reached the electron temperatures up to more than 450 eV and densities up to 2×10^{20} cm^{-3} on MAIZE LTD generator. In addition, despite the low mass of the loads, opacity effects were observed in the most prominent K-shell Al lines almost in every shot. For DPWAs, most of the intense K-shell lines were localized either near the cathode or close to both the cathode and anode, whereas for SPWA, K-shell lines filled almost the whole gap between the cathode and the anode. More work is in progress on the MAIZE LTD generator to understand

the inductance of the wire array loads and plasma evolution during their implosion and stagnation on university-scale LTD generators.

REFERENCES

[1] W. A. Stygar *et al.*, "Architecture of petawatt-class *z*-pinch accelerator," *Phys. Rev. Sepcial Topics Accel. Beams*, vol. 10, p. 030401, Mar. 2007.

[2] M. G. Mazarakis *et al.*, "High-current linear transformer driver development at Sandia National Laboratories," *IEEE Trans. Plasma Sci.*, vol. 38, no. 4, pp. 704–713, Apr. 2010.

[3] R. M. Gilgenbach *et al.*, "MAIZE: A 1 MA LTD-driven Z-pinch at the University of Michigan," in *Proc. AIP Conf.*, 2009, pp. 259–262.

[4] J. C. Zier *et al.*, "Magneto-Rayleigh–Taylor experiments on a MegaAmpere linear transformer driver," *Phys. Plasmas*, vol. 19, no. 3, p. 032701, 2012.

[5] V. L. Kantsyrev *et al.*, "Radiation properties and implosion dynamics of planar and cylindrical wire arrays, asymmetric and symmetric, uniform and combined X-pinches on the UNR 1-MA Zebra generator," *IEEE Trans. Plasma Sci.*, vol. 34, no. 2, pp. 194–212, Apr. 2006.

[6] V. L. Kantsyrev *et al.*, "Planar wire array as powerful radiation source," *IEEE Trans. Plasma Sci.*, vol. 34, no. 5, pp. 2295–2302, Oct. 2006.

[7] V. L. Kantsyrev *et al.*, "Double planar wire array as a compact plasma radiation source," *Phys. Plasmas*, vol. 15, no. 3, p. 030704, 2008.

[8] A. S. Safronova *et al.*, "X-ray diagnostics of imploding plasmas from planar wire arrays composed of Cu and few tracer Al wires on the 1 MA pulsed power generator at UNR," *Rev. Sci. Instrum.*, vol. 79, no. 10, p. 10E315, 2008.

[9] V. L. Kantsyrev *et al.*, "A review of new wire arrays with open and closed magnetic configurations at the 1.6 MA Zebra generator for radiative properties and opacity effects," *High Energy Density Phys.*, vol. 5, no. 3, pp. 115–123, 2009.

[10] K. M. Williamson *et al.*, "Implosion dynamics in double planar wire array Z pinches," *Phys. Plasmas*, vol. 17, no. 11, p. 112705, 2010.

[11] A. S. Safronova *et al.*, "Searching for efficient X-ray radiators for wire array Z-pinch plasmas using mid-atomic-number single planar wire arrays on Zebra at UNR," *High Energy Density Phys.*, vol. 7, no. 4, pp. 252–258, 2011.

[12] M. F. Yilmaz *et al.*, "Modeling of K-shell Al and Mg radiation from compact single, double planar and cylindrical alloyed Al wire array plasmas produced on the 1 MA Zebra generator at UNR," *High Energy Density Phys.*, vol. 8, no. 1, pp. 30–37, 2012.

[13] V. L. Kantsyrev *et al.*, "Radiation sources with planar wire arrays and planar foils for inertial confinement fusion and high energy density physics research," *Phys. Plasmas*, vol. 21, no. 3, p. 031204, 2014.

[14] A. S. Safronova *et al.*, "Radiation from mixed multi-planar wire arrays," *Phys. Plasmas*, vol. 21, no. 3, p. 031205, 2014.

[15] M. E. Weller *et al.*, "Radiation from Ag high energy density Z-pinch plasmas and applications to lasing," *Phys. Plasmas*, vol. 21, no. 3, p. 031206, 2014.

[16] A. S. Safronova *et al.*, "Radiative signatures of Z-pinch plasmas at UNR: From X-pinches to wire arrays," *Int. J. Modern Phys., Conf. Ser.*, vol. 32, p. 1460316, Aug. 2014.

[17] V. V. Shlyaptseva *et al.*, "Gold planar wire array radiation sources at university scale generators and their applications," *Int. J. Modern Phys., Conf. Ser.*, vol. 32, Aug. 2014, Art. no. 1460324.

[18] A. S. Safronova *et al.*, "First experiments with planar wire arrays on U Michigan's linear transformer driver," in *Proc. Bulletin 56th Annu. Meeting APS Division Plasma Phys.*, vol. 59. no. 15, Oct. 2014, p. 109. [Online]. Available: http://meetings.aps.org/link/BAPS.2014.DPP.G04.1

[19] A. A. Esaulov *et al.*, "Wire ablation dynamics model and its application to imploding wire arrays of different geometries," *Phys. Rev. E*, vol. 86, p. 046404, Oct. 2012.

[20] A. A. Esaulov *et al.*, "Magnetostatic and magnetohydrodynamic modeling of planar wire arrays," *Phys. Plasmas*, vol. 15, no. 5, p. 052703, 2008.

[21] J. P. Apruzese, J. W. Thornhill, K. G. Whitney, J. Davis, C. Deeney, and C. A. Coverdale, "Comparative analysis of time-resolved and time-integrated X-ray data from long pulse Z-pinch implosions on Saturn," *Phys. Plasmas*, vol. 8, no. 8, pp. 3799–3809, 2001.

[22] J. P. Apruzese *et al.*, "The physics of radiation transport in dense plasmas," *Phys. Plasmas*, vol. 9, no. 5, pp. 2411–2419, 2002.

[23] M. F. Gu, "The flexible atomic code," *Can. J. Phys.*, vol. 86, no. 5, pp. 675–689, 2008.

Alla S. Safronova (M'06) was born in Moscow, Russia. She received the Ph.D. degree in physics from the Institute of General Physics, Russian Academy of Sciences, Moscow, in 1986.

She was a Visiting Scientist and then a Post-Doctoral Research Associate with the Department of Physics, University of Nevada, Reno, NV, USA, from 1994 to 1998, where she has been an Associate Research Professor since 1998, and is currently a Research Professor. Her former Ph.D. students are with Sandia National Laboratories, Albuquerque, NM, USA, the Naval Research Laboratory, Washington, DC, USA, and also abroad at various universities. She is one of the pioneers in the application of X-ray line polarization to astrophysical and laboratory plasmas. Her current research interests include studying of radiation from and processes in high energy density plasmas, such as Z-pinch and high-power laser plasmas, and tokamak plasmas.

Prof. Safronova organized and co-chaired the series of international workshops on Radiation from High Energy Density Plasmas (RHEDP 2011, 2013, and 2015) as well as chaired sessions at ICOPS and other international meetings on plasma physics, and was the Guest Editor of the Fifth Special Issue on Z-Pinch Plasmas of the IEEE TRANSACTIONS ON PLASMA SCIENCE in 2012, and of the Special Topic Section on RHEDP of *Physics of Plasmas* in 2014.

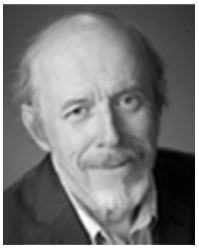

Victor L. Kantsyrev (M'06) received the M.S. and Ph.D. degrees from the Moscow Engineering Physics Institute, Moscow, Russia, in 1972 and 1981, respectively, and the D.Sc. (equivalent to the Dr. Habil. degree in Europe) degree from the Institute of Analytical Instrumentation, Russian Academy of Sciences, Saint Petersburg, Russia, in 1992.

He was a Researcher and the Head of sectors and laboratory in several Russian scientific institutes. He joined the Physics Department, University of Nevada, Reno, NV, USA, in 1994, where he has been a Research Professor since 1996. He was one of the pioneers in research on compact laser- and gas-puff plasma X-ray sources and their applications and the development of X-ray and extreme UV glass capillary optics. His former Ph.D. students are with Sandia National Laboratories, Albuquerque, NM, USA, and the Naval Air Warfare Center, China Lake, CA, USA. He has authored over 210 scientific papers (including two U.S. patents and five USSR Inventor's certificates). His current research interests include radiative properties and implosion dynamics of planar and cylindrical wire-arrays, planar foils, and X-pinch plasmas and their applications for radiation physics and inertial confinement fusion, pulsed power, high-power laser plasmas, and the plasma diagnostics.

Dr. Kantsyrev organized and chaired the technical areas and sessions at the International Conference on Plasma Science, the Pulsed Power Conference, and the International Society for Optical Engineers Conferences.

Michael E. Weller (M'14) was born in Visalia, CA, USA, in 1984. He received the B.S. degree in physics from Arkansas Tech University, Russellville, AR, USA, in 2007, and the Ph.D. degree in physics from the University of Nevada, Reno, NV, USA, in 2014, with a focus on theoretical and experimental physics related to Z-pinches.

He was a Post-Doctoral Scholar in physics related to Z-pinches with the University of Nevada after the graduation. He is currently a Post-Doctoral Research Staff Member with the Lawrence Livermore National Laboratory, Livermore, CA, USA.

Veronica V. Shlyaptseva (M'12) was born in Moscow, Russia, in 1984. She received the B.A. degree from the University of Nevada, Reno, NV, USA, in 2008.

She is currently a Staff Member with the University of Nevada. She is involved in X-ray diagnostics and spectroscopy of Z-pinch and laser plasmas and modeling of hohlraum experiments.

Ishor K. Shrestha was born in Gorkha, Nepal. He received the M.S. degree from Tribhuvan University, Kathmandu, Nepal, and the Ph.D. degree from the University of Nevada, Reno, NV, USA, in 2010.

He was a Lecturer in Physics with Tribhuvan University, Kirtipur, Nepal, for eight years. He is currently a Post-Doctoral Research Associate with the Department of Physics, University of Nevada. He has authored over 50 papers in scientific journals. His current research interests include hard X-ray polarimetry diagnostic development, laser plasma, wire arrays, and X-pinch research.

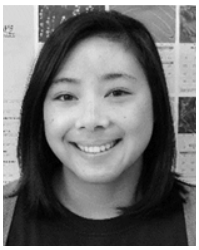

Mindy Y. Lorance was born in Honolulu, HI, USA, in 1992. She received the B.S. degree in physics from the University of Nevada, Reno, NV, USA, in 2015, where she is currently pursuing the M.S. degree.

She is involved in modeling X-ray radiation from Z-pinch plasmas.

Maximillian T. Schmidt-Petersen was born in Novato, CA, USA, in 1994. He is currently pursuing the B.S. degree in physics with a minor in mathematics with the University of Nevada, Reno, NV, USA.

He has been involved in both experimental and theoretical research, concerning wire array Z-pinch plasmas with a focus on studying implosion dynamics using magnetohydrodynamic simulations since 2014.

Austin Stafford was born in Upland, CA, USA, in 1987. He received the B.S. degree in physics and mathematics from Linfield College, McMinnville, OR, USA, in 2009. He is currently pursuing the Ph.D. degree with the University of Nevada, Reno, NV, USA.

He is involved in theoretical work on X-ray spectroscopy of Z-pinches with the University of Nevada.

Matthew C. Cooper was born in Las Vegas, NV, USA, in 1992. He received the B.S. degree in physics from the University of Nevada, Reno, NV, USA, in 2014, where he is currently pursuing the M.S. degree in physics.

He is involved in experimental work on vacuum spark and gas-puff Z-pinches and X-ray spectroscopy of these plasmas with the University of Nevada.

Adam M. Steiner (S'10) received the B.S. degrees in nuclear engineering and physics from North Carolina State University, Raleigh, NC, USA, in 2010, and the M.S. degree in nuclear engineering and radiological sciences from the University of Michigan, Ann Arbor, MI, USA, in 2012, where he is currently pursuing the Ph.D. degree in nuclear engineering and radiological sciences.

He is an Experimentalist with the University of Michigan, where he is involved in the physics of dynamic loads on linear transformer drivers and instabilities of Z-pinch plasmas.

David A. Yager-Elorriaga (S'13) received the B.A. degree in physics and mathematics with a minor in Spanish from Gettysburg College, Gettysburg, PA, USA, in 2010, and the M.S.E. degree in nuclear engineering and radiological sciences with a minor in plasma physics from the University of Michigan, Ann Arbor, MI, USA, in 2013, where he is currently pursuing the Ph.D. degree with a focus on pulsed power and mitigation of Z-pinch plasma instabilities under the guidance of Prof. R. M. Gilgenbach.

Dr. Yager-Elorriaga received a National Science Foundation Graduate Research Fellowship Program Fellowship in 2012.

Sonal G. Patel received the B.S. degree in astrophysics from Rutgers University, New Brunswick, NJ, USA, in 2015. She is currently pursuing the Ph.D. degree in nuclear engineering and radiological sciences with the University of Michigan, Ann Arbor, MI, USA.

She is with Sandia National Laboratories, Albuquerque, NM, USA, where she is involved in visible spectroscopy measurements of radiographic diodes.

Nicholas M. Jordan (S'05–M'13) received the B.S.E., M.S.E., and Ph.D. degrees from the University of Michigan (UM), Ann Arbor, MI, USA, in 2002, 2004, and 2008, respectively, all in nuclear engineering.

He was with Cybernet Systems, Ann Arbor, where he was involved in microwave vehicle stopping technology, for five years, before returning to UM as an Assistant Research Scientist with the Plasma, Pulsed Power, and Microwave Laboratory in 2013. His current research interests include high-power microwave devices, pulsed power, laser ablation, Z-pinch physics, and plasma discharges.

Ronald M. Gilgenbach (LF'15) received the B.S. and M.S. degrees from the University of Wisconsin–Madison, Madison, WI, USA, in 1972 and 1973, respectively, and the Ph.D. degree in electrical engineering from Columbia University, New York, NY, USA, in 1978.

He spent several years as a member of the Technical Staff with Bell Laboratories, Holmdel, NJ, USA, in the 1970s. From 1978 to 1980, he performed gyrotron research with the Naval Research Laboratory, Washington, DC, USA, and the first electron cyclotron heating experiments on tokamak plasma with the Oak Ridge National Laboratory, Oak Ridge, TN, USA. He joined as a Faculty Member with the University of Michigan (UM), Ann Arbor, MI, USA, in 1980, where he became the Director of the Plasma, Pulsed Power and Microwave Laboratory. He has collaborated in research with scientists at the Air Force Research Laboratory, Kirtland Air Force Base, NM, USA, Sandia National Laboratories, Albuquerque, NM, USA, NASA Glenn, Cleveland, OH, USA, Northrop Grumman, Rolling Meadows, IL, USA, L-3 Communications, San Carlos, CA, USA, General Motors Research Laboratories, the Los Alamos National Laboratory, Los Alamos, NM, USA, Fermilab, Batavia, IL, USA, the Naval Research Laboratory, the Institute of High Current Electronics, Tomsk, Russia, and many other universities. He is currently the Chair and Chihiro Kikuchi Collegiate Professor with the Nuclear Engineering and Radiological Sciences Department, UM. He has supervised 46 graduated Ph.D. students and has authored over 165 articles in refereed journals and books, and holds five patents granted at UM.

Dr. Gilgenbach is a fellow of the American Physical Society Division of Plasma Physics. He received the NSF Presidential Young Investigator Award in 1984 and the Plasma Sciences and Applications Committee (PSAC) Award from the IEEE in 1997, and served as the PSAC Chair from 2007 to 2008. He was an Associate Editor of the *Physics of Plasmas* journal.

Alexander S. Chuvatin, photograph and biography not available at the time of publication.